







Performance of Slope Behavior Indicators in Unsaturated Pyroclastic Soils


Luciano PICARELLI¹  <http://orcid.org/0000-0001-6670-1895>; e-mail: luciano.picarelli@unina2.it

Emilia DAMIANO¹  <http://orcid.org/0000-0001-8361-3694>;  e-mail: emilia.damiano@unina2.it

Roberto GRECO¹  <http://orcid.org/0000-0002-7380-4515>; e-mail: roberto.greco@unina2.it

Aldo MINARDO²  <http://orcid.org/0000-0002-8966-9143>; e-mail: aldo.minardo@unina2.it

Lucio OLIVARES¹  <http://orcid.org/0000-0003-0723-0872>; e-mail: lucio.olivares@unina2.it

Luigi ZENI²  <http://orcid.org/0000-0001-8356-7480>; e-mail: luigi.zeni@unina2.it

¹ Department of Civil Engineering, Design, Home Building and Environment, Seconda Università di Napoli, Aversa 81031, Italy

² Department of Industrial and Information Engineering, Seconda Università di Napoli, Aversa 81031, Italy

Citation: Picarelli L, Damiano E, Greco G, et al. (2015) Performance of slope behaviour indicators in unsaturated pyroclastic soils. *Journal of Mountain Science* 12(6). DOI: 10.1007/s11629-014-3104-3

© Science Press and Institute of Mountain Hazards and Environment, CAS and Springer-Verlag Berlin Heidelberg 2015

Abstract: Landslide risk is increasing in many parts of the world due to growth of population and infrastructures. Therefore, an effort has to be made in developing new and cheap sensors for areas susceptible of landslides to continuously control the slope behaviour, until approaching failure conditions. The paper reported experimental data from small-scale physical models about the performance of Time Domain Reflectometry (TDR) and optical fibres, which act as the indicators of the incoming failure of slopes covered by unsaturated granular soils. Obtained results appear encouraging, since both sensors provide continuous information about the state of the slope, in terms of water content profiles and ongoing deformations, induced by rainwater infiltration, even immediately before the triggering of a fast landslide.

Keywords: Unsaturated granular soils; Slope monitoring; Rapid landslide; Optical fibre; Time Domain Reflectometry; Probe

Introduction

In modern society, natural and anthropogenic risk is growing, because of an unavoidable increase in exposure. Among natural hazards, rainfall-induced landslides affect large areas worldwide and are responsible of huge losses, and the related hazard seems to increase due to climate change (IPCC 2011). A response to the societal demand of security requires the development of reliable criteria for risk mitigation, which can be achieved through active or passive works. Nonetheless, these measures are often impractical due to economic, morphological or environmental constraints.

Thanks to the development of new and accurate sensors and effective systems of timely data transfer, the demand for early warning systems is increasing as a useful measure for risk mitigation (Sassa et al. 2008; Picarelli et al. 2009). A crucial aspect of this approach is the capability to reliably predict location and occurrence of the

Received: 9 April 2014
Accepted: 4 February 2015

phenomenon in due time. Unreliable predictions, resulting in false or missing alarms, are still limiting the use of early warning systems (Gasparini et al. 2007).

Real-time prediction of landslide occurrence can be obtained through the monitoring of either the potential trigger or the slope response to such a trigger. For rainfall-induced landslides, precipitation, here indicated as the precursor, represents the trigger, while water content, pore pressure change, displacement and displacement rate can be regarded as indicators of the slope response.

Examples of operating early warning systems exist, some based on comparison of measured precipitations to empirical thresholds (Keefer et al. 1987; Wilson et al. 1993; Wiley 2000; Ortigao and Justi 2004), others on monitoring of indicators (Flentje et al. 2005). In some cases, integrated systems based on both monitoring of incoming precipitations and of changes in soil state are being used to establish different levels of warning (Brand et al. 1984; Iwamoto 1990; Baum et al. 2005; Chleborad et al. 2008). A recent review about operating early-warning systems in Europe is reported in Alfieri et al. (2012).

Shallow landslides are a typical consequence of extreme rainfall events, but the identification of empirical rainfall thresholds for the prediction of their triggering is rarely feasible, as historical rainfall data associated to slope failures are required. Such landslides usually occur along steep slopes covered with unsaturated granular deposits, as in the case of landslides which occurred during the last decades in the hilly area of Campania, Southern Italy (Calcaterra et al. 2004; Cascini and Ferlisi 2003; Crosta and Dal Negro 2003; Guadagno et al. 2005). Figure 1 shows the location of the largest landslides which occurred during the last decades. Here the involved slopes are covered with loose air-fall granular deposits originated by the eruptions of some volcanic complexes (Rolandi et al. 2003; Di Crescenzo and Santo 2005). In many cases, the failed soil mass attained a size of tens of thousands cubic metres and reached a velocity of metres per second (Faella and Nigro 2003). Such slopes are in equilibrium

thanks to the contribution of soil suction to shear strength, which allows stability of slopes steeper than the friction angle of the material (Olivares and Picarelli 2003). Owing to the rainfall infiltration, a landslide can be suddenly triggered, as the resisting force no longer balances the driving force. In fact, the increase of water content causes an increase of soil weight and a decrease of suction and associated cohesion (Fredlund and Rahardjio 1993).

The continuous monitoring of suction and/or of water content, as indicators of stability conditions, can therefore provide useful information. It is well known that these two variables are related through the non linear soil water retention curve (SWRC). Owing to the steep slope of the transition zone of the SWRC, near saturation small changes in suction correspond to great changes in water content. In the considered slopes, failure usually occurs in saturated or nearly saturated conditions. Monitoring data show that during the wet season, soil suction drops to very small values (Damiano et al. 2012; Sorbino and Nicotera 2013) of a order of a few kPa, while water content still remains far below saturation (Greco et al. 2014; Pirone et al. 2014). Thus, monitoring of water content seems more suitable than suction to reveal the incoming failure.

Traditional monitoring performed with

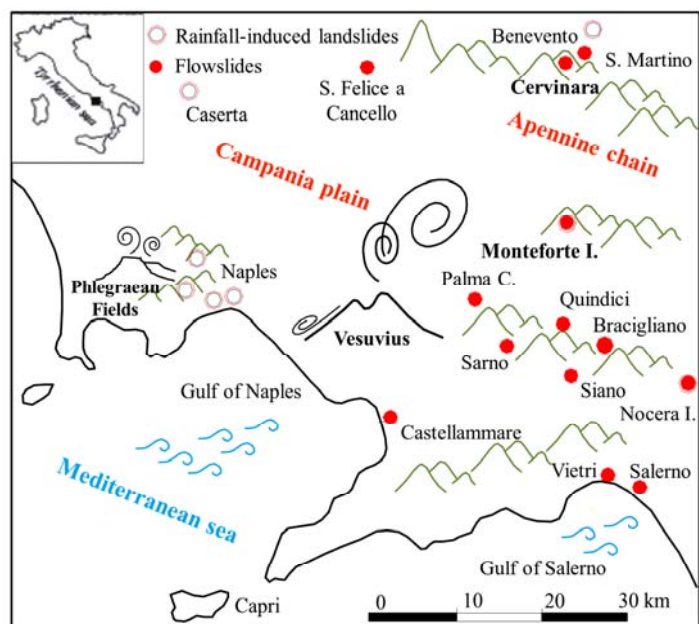


Figure 1 Rainfall-induced landslides occurred in Campania during the last century.

inclinometers, topographic or photogrammetric surveys are generally useless. In fact, such monitoring devices are suitable to monitor slow moving landslides, while shallow landslides in loose unsaturated granular soils usually show significant soil deformations only a short time before failure. In fact, when suction becomes very small, due to unusual precipitation, loose soils experience a strong decrease in the void ratio, denoted as volumetric collapse (Olivares and Picarelli 2003; Olivares and Damiano 2007), and tensile cracks develop along the slope, owing to shear strain (Olivares and Picarelli 2006; Picarelli 2009). Adopting sensors, like optical fibers, capable of detecting in real time such soil deformations which can appear everywhere along the slope, could be another useful tool to predict the impending event. So far, optical fibers have been adopted for the monitoring of deep-seated landslides (Iten and Puzrin 2009).

Hence, *in situ* monitoring of water content along the soil profile and of soil deformations along some slope sections could realize an effective early-warning system for prediction of shallow rapid landslides in pyroclastic soils, since the significant changes exhibited by such variables approaching failure, allow to adopt them as early indicators of failure.

The aim of this study is to assess, through investigation on small scale model slopes, the reliability of Time Domain Reflectometry (TDR) probes, to measure soil water content, and of optical fibres, to detect soil deformation, to realize such an early warning system in slopes covered with unsaturated pyroclastic deposits.

1 Materials and Methods

1.1 Hydraulic and mechanical properties of air-fall ashes

Figure 2 reports the grain size of the air-fall volcanic ashes, taken at Cervinara and Monteforte Irpino (Figure 1), used in the experiments described below. These two slopes, like many others in the area, are covered with a few meters of pyroclastic soils, resting upon a fractured limestone bedrock. The covers are layered, with alternating layers of ashes and pumices, and

sometimes altered ashes located at the bottom of the profile (Damiano et al. 2012; Pirone et al. 2012). The two investigated soils belong to ashy layers, which, as most of the similar deposits in Campania, consist of non plastic silty sands. Their porosity is quite high, ranging between 65% and 75%.

The water retention curves of both deposits, obtained during infiltration experiments in small-scale model slopes, are shown in Figure 3. The curves display a low air entry value (3-5 kPa) and a steep slope in the transition zone. More details about the water retention properties of the investigated materials can be found in Damiano and Olivares (2010) and Sorbino and Nicotera (2013).

The hydraulic conductivity of the Cervinara ash ranges between 10^{-6} and 10^{-8} m/sec, moving from a fully saturated condition to a degree of

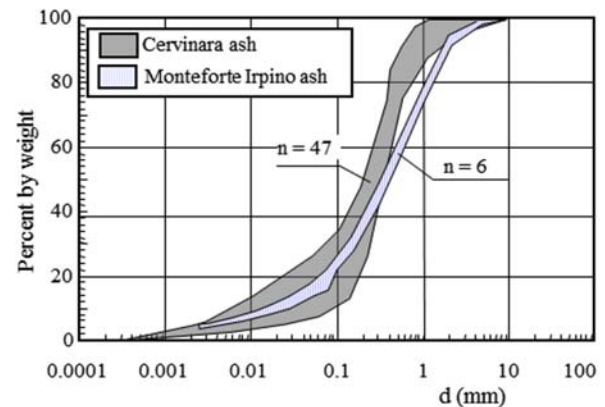


Figure 2 Grain size of Cervinara and Monteforte Irpino volcanic ashes (n = number of determinations) (modified after Damiano et al. 2012).

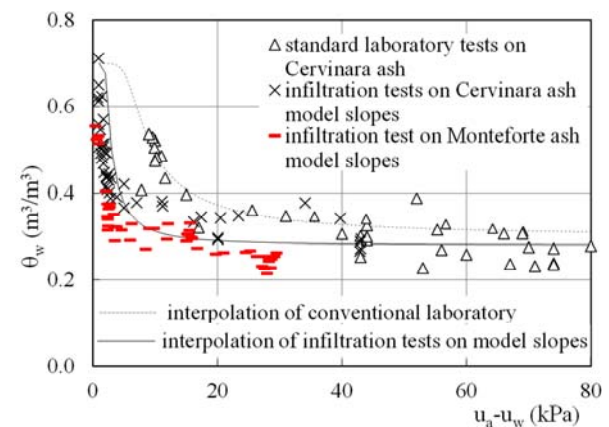


Figure 3 Water retention curves of Cervinara and Monteforte Irpino ashes (modified after Damiano and Olivares 2010).

saturation of about 40% (Olivares and Picarelli 2003). More data concerning the Monteforte Irpino ash, which displays similar values, are reported by Papa et al. (2010).

The friction angle of the Cervinara and Monteforte Irpino ash is respectively 38° and 37° . Both soils show a negligible effective cohesion. Nonetheless, in unsaturated conditions, the apparent cohesion can grow up to more than 10 kPa as a function of soil suction (Olivares 2001; Sorbino and Nicotera 2013). The deformability is quite high, owing to the high void ratio. As a consequence, significant volumetric strain (volumetric collapse) has been observed as the soil approaches saturation.

1.2 Flume experiments to test the proposed indicators

The aim of the research is to test a system based on two low-cost sensors of volumetric water content and strain, TDR probes (Topp et al. 1980) and optical fibers (Niklès et al. 1997), to check its suitability as an early-warning system for rainfall-induced landslides in pyroclastic soils. The system has been tested through infiltration experiments in an instrumented flume where small-scale slopes have been subjected to rainfall until failure.

The flume has a length of 1.9 m, a width of 0.5 m and a depth of 0.5 m. The slope inclination can reach an angle of 65° . The bottom of the flume allows to reproduce either pervious or impervious

soil-bedrock interface. The slope can be instrumented with minitensiometers (range 0-80kPa; sensitivity 1 kPa), pore pressure transducers (range 0-3.5 kPa; sensitivity 0.035 kPa), TDR probes, laser transducers (range 0-100 mm; sensitivity $20 \mu m$) to measure settlements at ground surface, optical fibres. TDR probes and optical fibres are described in detail, in the following sections. A rain gauge, located at the toe of the slope, and a standard thermocouple, buried in the soil near the bottom of the flume around its centre, allow measurement of rainfall intensity and soil temperature during the tests. A sketch of the instrumented flume is shown in Figure 4. The position of the devices in the plan-view of Figure 4c is approximate; for each experiment the exact locations of the transducers and minitensiometers are given in Table 1. More details regarding equipment and testing procedures can be found in Olivares et al. (2009).

Several tests have been performed with the two described ashes, reconstituted at different soil porosities, various initial conditions and applied rainfall intensities (Greco et al. 2010). The results of three tests are shown in the following sections. To obtain uniform porosity and water content, the soil is laid down by the moist-tamping technique, in thin layers of around 0.5 cm. During formation of the slope, two strands of the same single-mode standard optical fibre are buried in the soil, at the middle of the layer, in the longitudinal direction of the flume (Figure 4a). The excess length of fibre

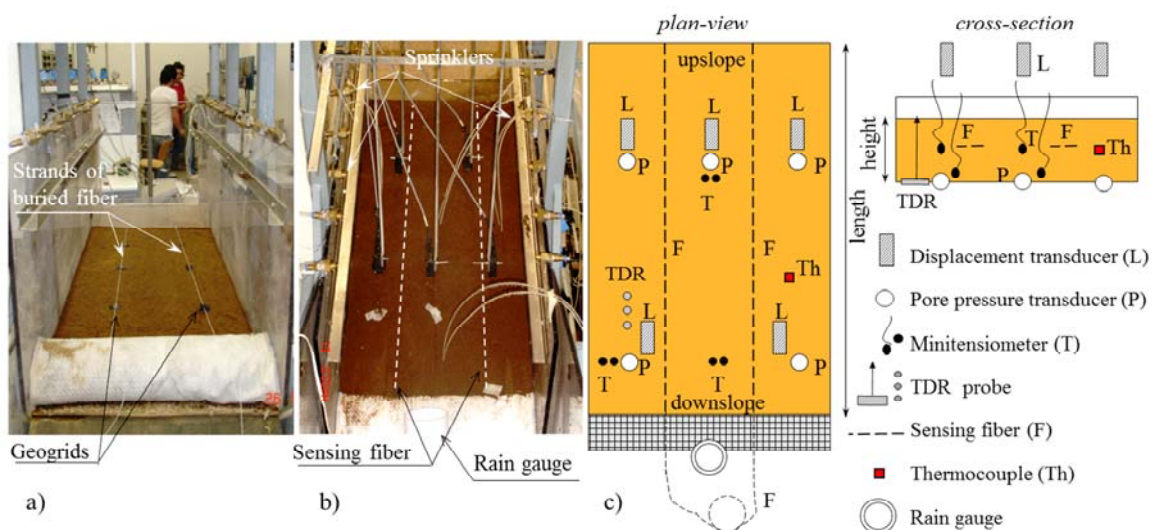


Figure 4 Equipment for experiments on small-scale unsaturated slopes: a) installation of the optical fiber during the reconstitution of the soil deposit; b) the instrumented model slope at the beginning of the test; c) schematic plan-view and cross-section of the monitoring system.

Table 1 Position of the sensors during each flume experiment

Test	Upslope section	Downslope section	Superficial	Deep	TDR probe	Optical fiber	Geogrid
A	L2, L4 T2, T4, T5, T6, T7 P1, P2, P5	L1, L3, L5 T1 P3, P4	- T1, T4, T6 -	- T2, T5, T7 -	yes (downslope)	yes	no
B	L1, L2, L4 T1, T2 P1, P4, P5	L3, L5 T3, T4, T6 P2, P3, P6	- T2, T3, T6 -	- T1, T4 -	yes (downslope)	no	no
C	L3, L5 T4, T6 -	L1, L2, L4 T2, T5, T7 -	- T6, T7 -	- T2, T4, T5 -	no	yes	yes

Notes: L = Laser sensor; T = Tensiometer; P = Pore pressure transducer.

Table 2 Main characteristics of the tests

Test	Soil	z (m)	l (m)	α (°)	n_o	$(u_a - u_w)_o$ (kPa)	Sr_o	i (mm/h)
A	Monteforte Irpino	0.1	1.10	40	0.74	15	-	45
B	Cervinara	0.1	1.20	40	0.76	41	0.33	56
C	Cervinara	0.1	1.35	38	0.73	41	0.44	50

Notes: z = Thickness; l = Length; α = Slope angle; n_o = Initial soil porosity; $(u_a - u_w)_o$ = Initial mean suction; Sr_o = Initial degree of saturation; i = Rainfall intensity.

between the two buried strands is placed outside the slope. After formation of the deposit, minitensiometers and a TDR probe are inserted, and the surface is covered by a plastic membrane to prevent evaporation and attain an equilibrium condition. Then the flume is tilted to the established slope angle and the test starts. The experiments are conducted by imposing constant artificial rainfalls. The applied intensities reported in Table 2 have been chosen in order to limit the duration of the experiments around one hour. Such intensities ranging between 45 and 56 mm/h are not necessarily representative of real events, as the aim of the experiments is only testing the capability of the system to detect incoming failure, rather than reproducing the evolution of a real event usually lasting for 24-48 h (Pagano et al. 2010; Damiano et al. 2012).

The main characteristics of the three described tests are reported in Tables 1 and 2. As indicated in Table 1, the minitensiometers, the laser and the pore pressure transducers are grouped into two nests indicated as upslope (0.3-0.5 m from the top of the flume) and downslope (0.8-1.0 m from the top of the flume). The minitensiometers are placed at a depth of 0.05 m (superficial) and 0.1 m (deep) below the ground surface. The TDR probe is inserted normally to the

flume bottom and crosses the entire deposit. Pore pressure transducers are located at the base of the deposits whereas the laser transducers are located above the ground surface, with the optical axis perpendicular to it.

1.3 Time Domain Reflectometry (TDR)

The TDR technique has been applied for a long time to investigate the mean volumetric water content of the soil. The experimental device consists of an electromagnetic pulse generator connected, through a coaxial cable, to a metallic probe a few decimetres long, buried under the ground surface. An electromagnetic pulse is sent through the soil, and the reflected signal is acquired. The speed of electromagnetic waves propagating through soil depends on its bulk dielectric permittivity, ϵ_r , while the attenuation of the signal mainly depends on bulk electrical conductivity, σ . Both variables are in turn related to volumetric water content, θ (Campbell 1990): the $\epsilon_r(\theta)$ and $\sigma(\theta)$ relationships can be experimentally determined in the laboratory. Measuring the travel time of the electromagnetic pulse provides the average bulk soil dielectric permittivity within a cylinder of soil coaxial to the probe. As a consequence, the mean volumetric

water content is obtained, with an average error of $\pm 0.02 \text{ m}^3/\text{m}^3$ (Topp et al. 1980).

Quite recently, a novel interpretation technique has been developed (Greco 2006; Greco and Guida 2008), which allows the inverse determination of the entire volumetric water-content profile along the metallic probe. The spatial resolution of the retrieved water content profile depends on the rise time of the electromagnetic pulse transmitted through the soil along the metallic probe. With the commonly adopted measurement devices, such a resolution is around 2 cm. Such a technique is based upon the numerical integration of the transmission line equations, which describe the electromagnetic transient along the probe (Ramo et al. 1994). By minimizing the difference between the experimental TDR wave traces and the simulated wave traces, the distributions of bulk soil dielectric permittivity and electrical conductivity are obtained. The empirical relationships linking volumetric water content with bulk soil dielectric permittivity and electrical conductivity, which are obtained in the same way as for usual TDR measurements, allow estimation of the volumetric water content.

Such a method allows use of longer probes than usual. In fact, measurement of the travel time requires the reflection of the electromagnetic wave at the end of the probe to be clearly detectable in the wave trace. Signal attenuation along the probe, mainly due to ionic electrical conductivity through soil water, reduces the amplitude and the steepness of the final reflection, making it very difficult to precisely locate the reflection time. As a consequence, especially for high water contents, the measurements based on the detection of travel time cannot be carried out with probes longer than 20 to 30 cm. The described interpretation technique, instead, exploits the information about water content distribution provided by signal attenuation and can detect the reflection at the end of the probe even when it is extremely smoothed. Indeed, it has been successfully applied with probe lengths of 40 cm both in the laboratory (Greco 2006) and in the field (Greco and Guida 2008). Acquisition of a TDR

wave trace takes a few seconds, while the calculations for water content profile retrieval take a few minutes, thus real-time measurements can be obtained frequently. The knowledge of the water content profile over the entire soil thickness allows estimating the incoming saturation, better than with point measurements. For field applications, with cover thickness of few meters, the use of several TDR probes buried at various depth is required for the estimation of the water content profile.

In the following sections, the use of TDR will be shown for the case of controlled infiltration experiments in small scale homogeneous model slopes. In this case, it is possible to assume a priori that soil water content monotonically grows upward, thus allowing to adopt the interpretation approach of Greco (2006), based on the use of a single TDR probe normal to the slope bottom. It has three metallic rods (diameter 3mm; spacing 1.5cm) and a length of 10cm, thus crossing the entire soil deposit.

Pyroclastic soils consist of light vesiculated (vesiculated) fragments with a wide range of particle sizes (from gravel to clay) characterised by internal voids, often unconnected, resulting in very low bulk densities, as shown in Table 3. Thus, specific experiments were performed to estimate the calibration relationship $\epsilon_r(\theta)$ for Cervinara ash (Greco et al. 2010). In Figure 5 the obtained experimental relationship is compared to the “universal” curve proposed by Topp et al. (1980) and to those proposed by Regalado et al. (2003) for other pyroclastic materials. One of the plotted curves for pyroclastic soils is very close to the one characterising the Cervinara ash. This result is probably due to the very low density of volcanic soils, which strongly affects the $\epsilon_r(\theta)$ relationship, as reported in literature (e.g., Malicki et al 1996). Adopting the relationship proposed by Topp et al. would lead to an underestimation by 10-20% of

Table 3 Physical, mechanical and hydraulic properties of investigated soils

Parameters	Cervinara	Monteforte Irpino
Specific weight of solid particles	2.59÷2.64	2.57
Bulk dry density (g/cm ³)	1.4÷1.5	1.4
Porosity	0.71÷0.74	0.71
Saturated hydraulic conductivity k_{sat} (m/s)	$1 \cdot 10^{-7} \div 5 \cdot 10^{-7}$	$7 \cdot 10^{-7}$
Effective friction angle ϕ' (°)	38	37
Cohesion c' (kPa)	0	0

the volumetric water content.

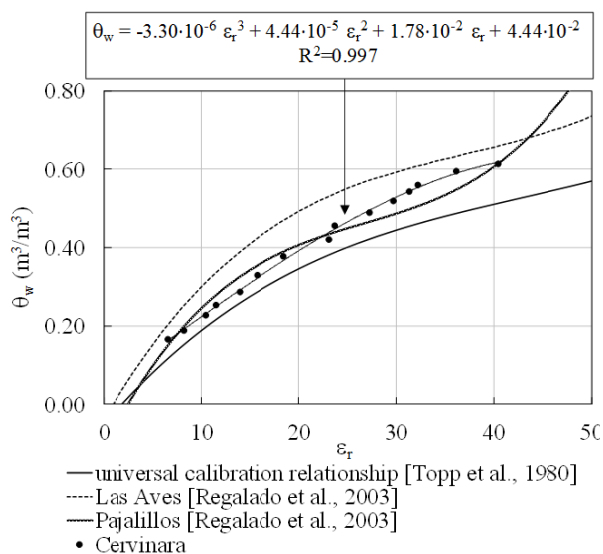


Figure 5 Volumetric water content vs. dielectric permittivity, ϵ_r , relationship for Cervinara ash (modified after Greco et al. 2010).

1.4 Optical fibre

Monitoring by optical fibres is performed by stimulated Brillouin scattering (SBS), which allows distributed temperature and strain readings along a single-mode optical fibre through Brillouin shift measurements. The measurement scheme involves the interaction between a pulsed pump beam and a counter-propagating continuous wave probe beam at a different wavelength. Positional information is obtained through a time-domain analysis; shorter pulses increase the spatial resolution.

A recent application of optical fibres is the monitoring of deformations of structures. Typically, the fibre is glued to the structure whose strains can be measured through analysis of the response of the fibre which follows any deformation of the structure. This technique, properly modified, seems also effective for measuring soil deformations (Picarelli and Zeni 2010). These are useful indicators of the slope

behaviour, since failure is generally preceded by soil strains large enough to be detected.

Other instruments and methods are currently used for monitoring of soil deformation, but they are not as cheap as optical fibre and can measure only local soil strain, so they are suitable when the failure surface is clearly identifiable. The advantage of the distributed optic sensing technique is in fact the possibility of deriving useful information about slope behaviour wherever the soil around the fibre is subjected to strain. Since the fibre cost is extremely low and the attenuation of the signal propagating along it is very small, it can be buried into the soil over even very long distances.

The equipment used in the experiments (Figure 6) includes: a first electro-optic modulator (IM1), which generates the continuous wave probe signal by the sideband technique (Niklès et al. 1997), a second electro-optic modulator (IM2), which provides pulses with widths down to 2 ns, and a detector, which consists of an InGaAs photo-detector and a preamplifier. After acquisition, data are processed by a standard Lorentzian fitting technique. Since acquisition and processing take a few minutes, the system can provide an updated deformation distribution every about 4 minutes. The deformation range is related to the tensile strength of the optical fiber cable employed for the tests (about 2%), while the resolution is in the order of 10 $\mu\epsilon$. As regards temperature effects, we must consider that a variation of 1 MHz of the Brillouin frequency shift is associated to either a temperature change of 1°C or a strain change of about 20 $\mu\epsilon$. For the

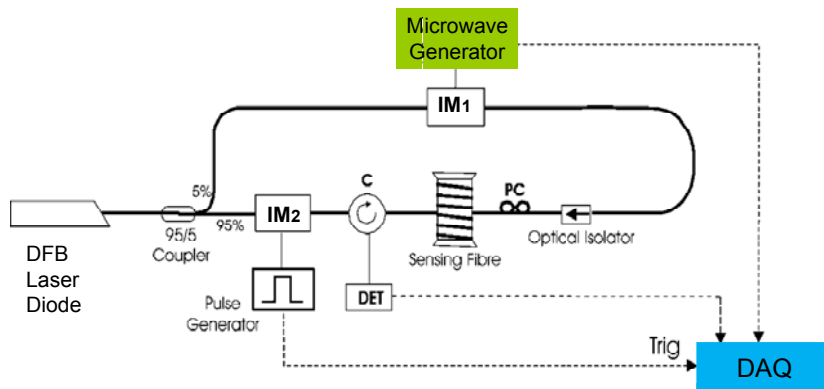


Figure 6 Experimental set-up for stimulated Brillouin scattering (SBS)-based fibre-optics measurements (IM1, IM2 = electro-optic modulators; C = optical circulator; PC = polarization controller; DET = detector, DAQ = data acquisition system).

experimental tests shown in this manuscript, the Brillouin frequency shift variations are in the order of tens or even hundreds of MHz, so the temperature effect can be considered as negligible.

2 Results and Discussion

In the following, the results of the flume tests reported in Table 2 are illustrated. First, the behaviour of the slope physical models during the early infiltration stage is described, then the response of the tested system is analyzed in more

detail when the slope approaches failure conditions.

As an example of the typical behaviour of loose deposits, Figures 7 and 8 report the evolution of suction, pore pressure, and displacements normal to the ground surface during tests A and B, respectively (Olivares et al. 2009). During test A, after the time needed for the wetting front to reach the depths of the installed tensiometers, a fast reduction of soil suction is observed. When the value of around 2kPa is reached along the entire soil profile, ground settlements start (Figure 7b). Afterwards, while

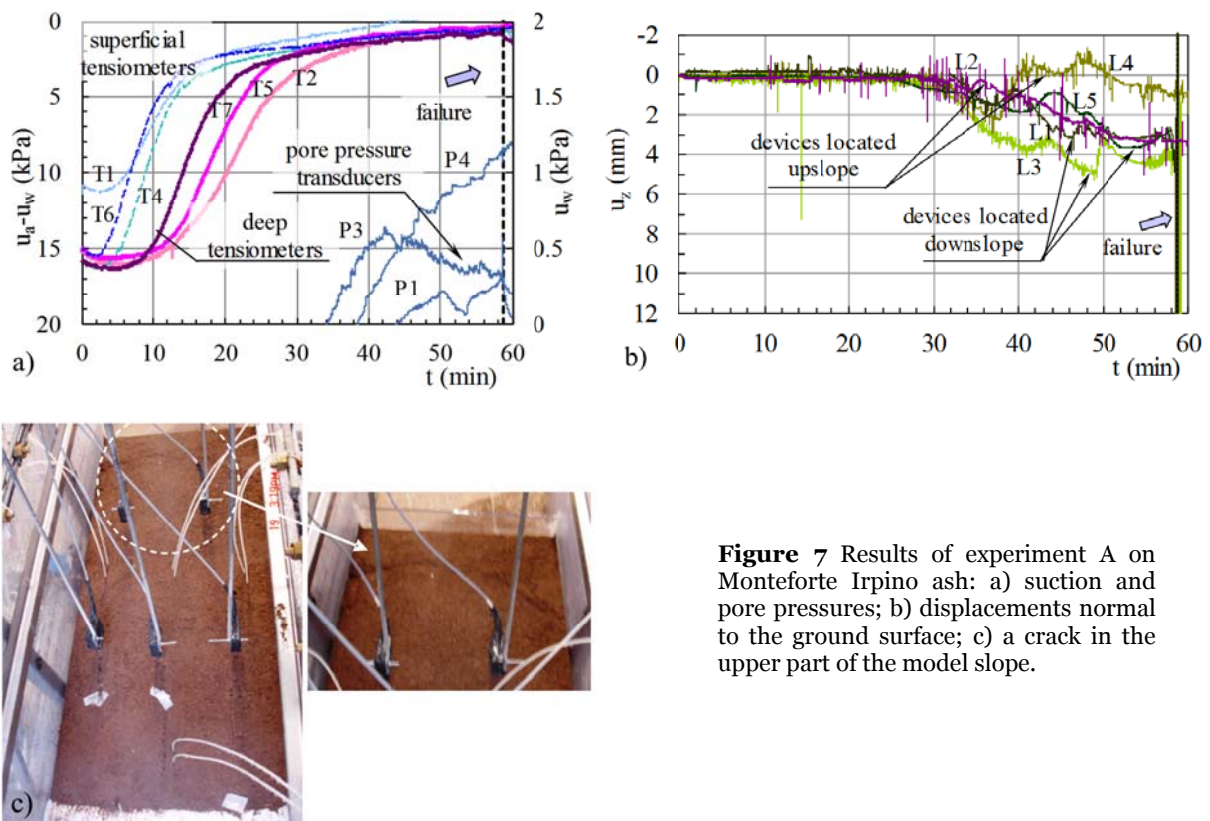


Figure 7 Results of experiment A on Monteforte Irpino ash: a) suction and pore pressures; b) displacements normal to the ground surface; c) a crack in the upper part of the model slope.

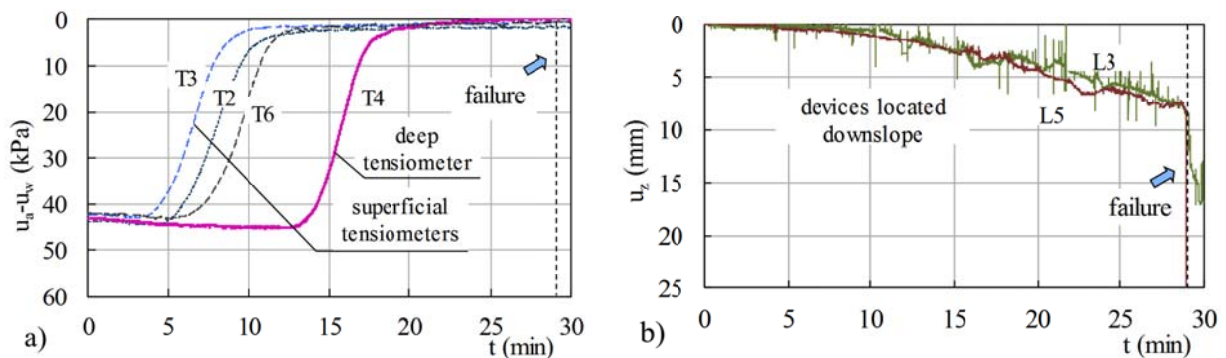


Figure 8 Results of experiment B on Cervinara ash: a) suction; b) displacements normal to the ground surface.

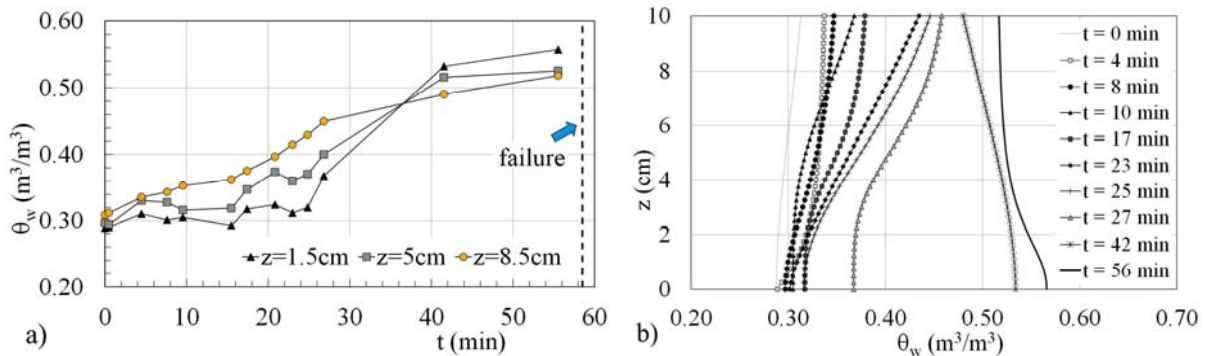


Figure 9 Volumetric water content measurements during test A: a) time history at three elevations; b) volumetric water content profiles.

slope deformations continue and some cracks develop in the upper part of the slope (Figure 7c), the observed reduction of soil suction becomes very slow, until the slope failure, which occurs about 58 minutes after the beginning of the infiltration process. A similar behaviour has been observed not only during test B, as shown by Figure 8, but also during all the other infiltration tests (Greco et al. 2010).

For test A, the time history of volumetric water content at three different depths is shown in Figure 9a. It looks clear that, once the wetting front reaches the considered depth, the increment of volumetric water content is much more gradual than the contemporary suction decrease. It is worth noting that in the last part of the experiment the soil at the bottom of the deposit becomes wetter than above, indicating that a water ponding is forming at the bottom, as confirmed by the readings of the pore pressure transducers (Figure 7a).

Figure 9b reports some volumetric water content profiles obtained from TDR readings. While the limited spatial resolution and accuracy of the TDR technique does not allow revealing the wetting front during the early stage of infiltration, in the profiles retrieved after 8 minutes and later, the downward propagation of the wet front becomes more and more evident. In particular, the profiles obtained between 17 and 27 minutes after the beginning of the experiment are quite in a good agreement with the values of suction, showing a decrease of the water content from the top to the bottom. In such a phase, the soil remains far from saturation, as the wetter part of the profile retrieved after 27 minutes reaches a saturation degree of 62% calculated in the

assumption of constant porosity. Unfortunately, for 15 minutes the TDR device did not work properly, so the following profile, acquired 42 minutes after the beginning of the experiment, looks more uniform, with an average volumetric water content around 50% (corresponding to a saturation degree higher than 70%). The last profile, recorded 3 minutes before failure, does not reach the hypothetical maximum value of 0.74. Considering the positive value of pore pressure, that indicates the attainment of full saturation at the bottom (Figure 7a), this result may indicate the occurrence of volumetric collapse, leading to a reduction of soil porosity. Such a remark is confirmed by the settlements at the ground surface and by the opening of a large crack as wide as the slope (Figure 7c).

The profiles of the volumetric water content retrieved during test B are reported in Figure 10. Again the figure shows the progressive downward advancement of the wetting front. About 20 minutes from the start, the slope reaches nearly uniform water content, but during the last 5 minutes the profiles present a different shape. In

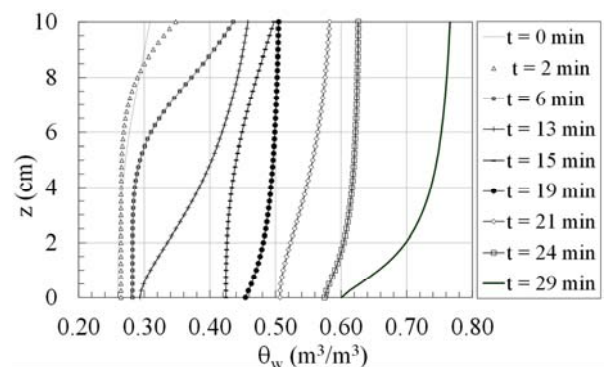


Figure 10 Volumetric water content profiles during experiment B.

particular, the last two profiles reveal that, in the upper part of the deposit, the saturated volumetric water content is being approached (the initial porosity is 0.76). In depth, instead, the profile shows smaller values of water content, which, at the bottom, attains only 0.6. Also in this case, this result can be ascribed to the volumetric collapse. In fact, the final average volumetric water content is around 0.73. Assuming that the last retrieved profile refers to nearly saturated conditions, and considering that during this test no significant crack appeared along the slope, the reduction of 0.03 with respect to the initial porosity can be interpreted as a measurement of the volumetric strain. Such a value is quite in a good agreement with soil strain estimated from the settlements of the ground surface, which reaches nearly 4mm just before failure (Greco et al. 2010).

Results of monitoring using optical fibres are reported in Figures 11 and 12 for the experiments A and C, respectively. In both the figures, the buried sections of the fibers are indicated by grey areas. The measurements reported in Figure 11a show a progressive increase in the shift frequency along the buried part of the fibre, which can be ascribed solely to a tensile strain increase, due to slope deformation, as soil temperature measured at the base of the slope remains constant during the experiment. Conversely, the decrease in the Brillouin shift frequency along the free spoil exposed to rain water in between the two buried

strands is caused by the cooling due to fibres wetting. The estimated decrease in temperature, based on its correlation with the Brillouin shift frequency, is about 8°C. Figure 11b shows steadily increasing tensile strain measured by the second strand since the beginning of the test. The magnitude of the increase (about 8 MHz) indicates a strain of about 0.016% along the direction of the slope. Such a value is two orders of magnitude smaller than soil deformation normal to the slope, as estimated from ground settlements. Although the two components of deformation could be significantly different, this mismatch is probably due to the imperfect connection between the fibre and the soil, which allows relative displacements. Similar results were obtained in experiment B.

The quality of readings can be improved by using geogrids to avoid relative movements between fiber and soil. With this respect, Figure 12 reports pre-failure strains measured during test C. The profile at t=0 (Figure 12a) indicates an initial deformation, accumulated during previous infiltration phases, carried out before the beginning of test C. In this case the increase in Brillouin frequency shift is about 250 MHz, corresponding to a strain, measured just before rupture, of 0.5%, i.e. more than one order of magnitude higher than the value of 0.016% measured in experiment A (Figure 11b), when a slip between the soil and the fiber occurred,

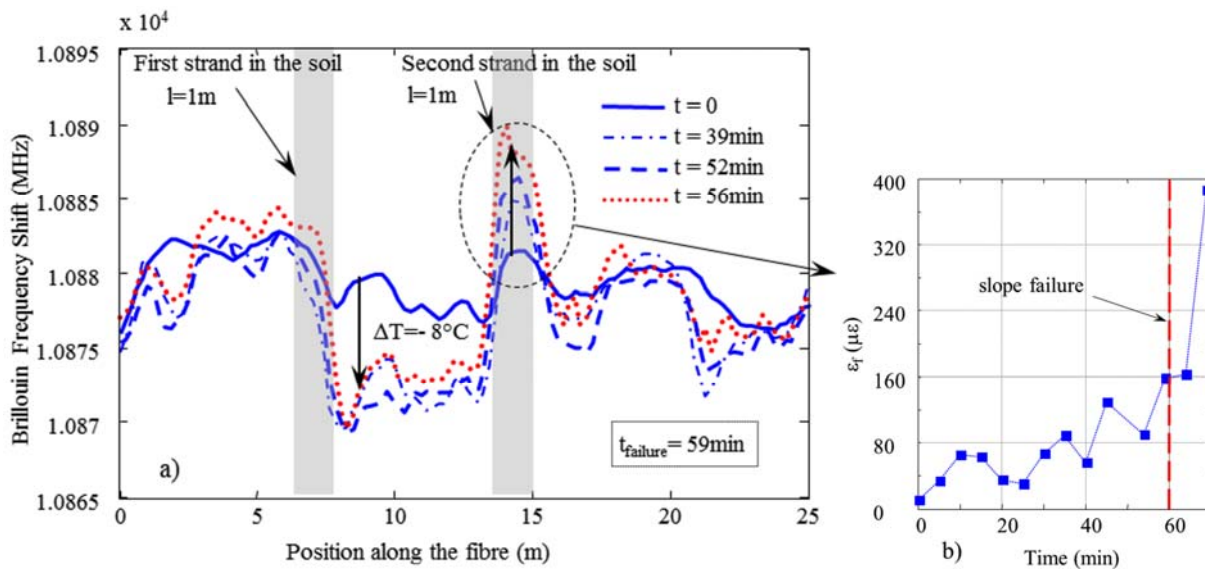


Figure 11 Experiment A: a) changes in the Brillouin shift frequency along the fibre; b) changes in the mean Brillouin frequency shift vs. time along the right strand.

hampering the capability of the fiber to detect the real displacements experienced by the soil. Further readings carried out after the sliding of the soil mass ($t > t_f$) show a complete strain recovery. The temporal evolution of strain reported in Figure 12b shows that few minutes before failure the fibre undergoes a sharp increase in tensile strain due to the formation of a crack normal to the slope direction (Figure 12c). This is a clear demonstration of progressive slope deformation accompanying ongoing failure. The progressive decrease of strain, observed during the last three minutes before slope failure, is again caused by the relative movement between soil and fiber, which, in presence of geogrids, occurs only at large deformation.

3 Conclusions

The occurrence of precipitation-induced landslides in granular pyroclastic soils is anticipated by mechanical processes that include increase in soil water content, typically characterised by the advancement of a wetting front in the subsoil, and deformations, that in very loose unsaturated soils include both volumetric and shear strains. Detection of such phenomena can be used in early warning systems of slope failure.

Aim of this paper is to check the reliability of a system constituted by TDR probes and optical fibers, which can be implemented in an early-warning system for rapid landslides. Such a scope is addressed by means of laboratory experiments, carried out in small scale model slopes, in which TDR sensors are used for monitoring of water

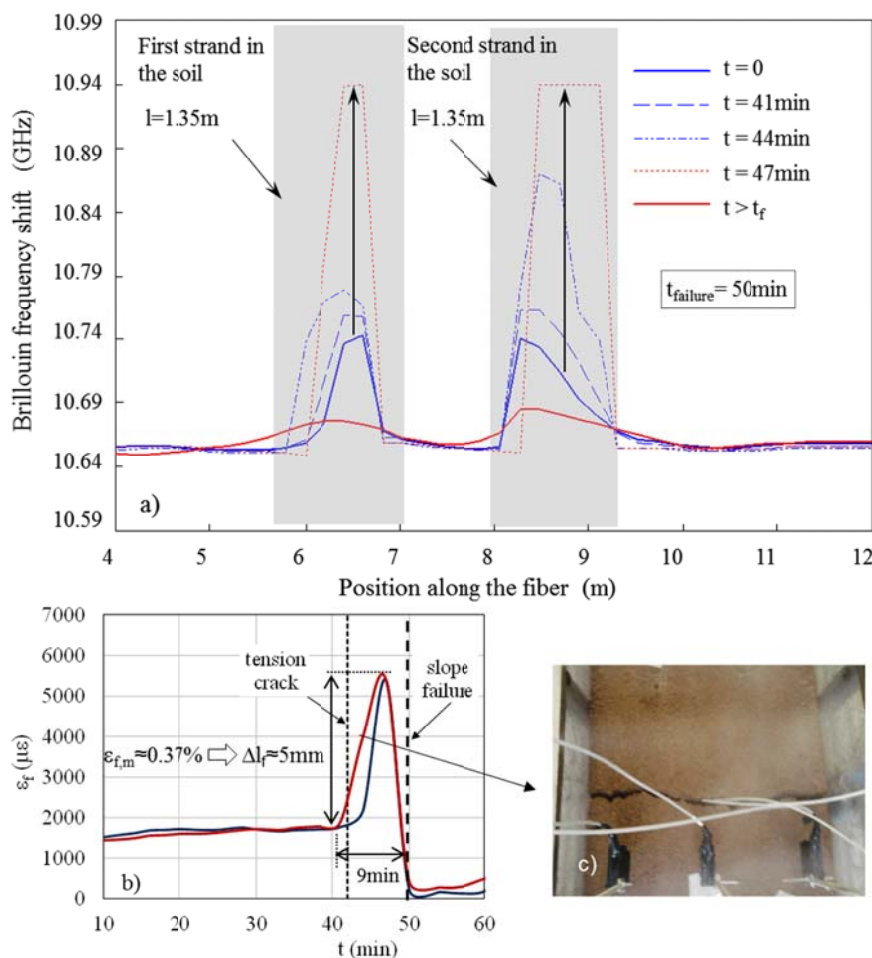


Figure 12 Experiment C: a) changes in the Brillouin shift frequency along the fibre; b) temporal evolution of the strain measured along the two strands of the fibre; c) the detected tension crack.

content vertical profiles, and optical fibres are adopted to capture pre-failure strains.

The reported experiments provide useful elements about the performance of the proposed system, suggesting that it can be used for monitoring and analysis of indicators of potential slope failure also in the field.

The TDR device is not a novelty as such, since it has been used for a long time to measure the average volumetric water content of the soil. However, the proposed data analysis, based on the knowledge of profiles of the volumetric water content covering the entire deposit, can be adopted also in the field, without substantial increase of cost and complexity, by burying several probes at various depths (Greco and Guida 2008; Comegna et al. 2013; Greco et al. 2013).

In all laboratory experiments the water content profiles proved to be consistent and reliable. In particular, obtaining continuous profiles of the volumetric water content along the entire rod length represents a significant improvement of the quality of monitoring. In addition, elaboration of data takes only a few minutes and readings can be automatically acquired. If probes are installed at different depths from the ground surface, this can contribute to a correct spatial and temporal interpretation of the evolution of the infiltration process from the ground surface. In fact, the probes clearly show the advancement of the wetting front in the early stage of infiltration. Afterwards, owing to the non linearity of the water retention curve, the gradual saturation of the soil can be better detected in terms of water content rather than with tensiometers. Therefore, they can provide useful information about the slope behaviour, as the volumetric collapse of loose soils close to full saturation. In addition, based on water retention curves, volumetric water content profiles can provide the fundamental information of distribution of suction with depth for slope stability analysis in unsaturated soils.

Of course, further investigations are required to check the reliability of the device in more complex field conditions, in which stratigraphy and heterogeneities in the soil properties play a significant role.

The use of optical fibres for monitoring of distributed soil strains is quite a novel technique, since most of the documented applications have been limited to structures or to structural elements embedded in the soil. Laboratory tests show that the fibre can be directly put into the soil. By adopting simple solutions to avoid relative displacements at the fibre-soil interface, internal soil deformation due to tension cracks, volumetric collapse or shear banding can be easily detected.

References

- Alfieri L, Salamon P, Pappenberger F, et al. (2012) Operational early warning systems for water-related hazards in Europe. *Environmental Science & Policy* 21: 35-49. DOI: 10.1016/j.envsci.2012.01.008
- Baum RL, Godt JW, Harp EL, et al. (2005) Early warning of

In particular, cracking can be induced by either volumetric collapse or by local shear strains.

The results of experiments on small-scale model slopes are encouraging. In such experiments, the first deformations were detected early, when the increase in the degree of saturation was only 10%. This confirms that such a technique could be very useful in loose soils which are susceptible to catastrophic landslides, where the volumetric deformation process starts quite early and could be detected in time to issue warnings. Also in this case, data elaboration takes few minutes and readings can be automatically stored or remotely transmitted. A prominent feature of this sensor is its ability to monitor distributed strains all along the fibre. This can help in detecting pre-failure deformations wherever they occur. In field applications, optical fibres can be directly laid in small trenches parallel or normal to the slope over long distances. If necessary, they can be protected from damage by installation inside small-diameter plastic tubes. In any case, reinforced fibres are now available, minimizing the risk of damage during installation.

In conclusion, the proposed system could represent a useful tool for timely alerting landslide triggering, especially if integrated with other devices. Data from different sensors can provide a complete and robust framework for the evaluation of the hydrological slope response, reducing the probability of missing or false alarms.

Acknowledgements

The work described in this paper was partially supported by the project SafeLand "Living with landslide risk in Europe: Assessment, effects of global change, and risk management strategies" under Grant No. 226479 (7th Framework Programme).

- landslides for rail traffic between Seattle and Everett, Washington, U.S.A. In: *Proceedings of an International Conference on Landslide Risk Management* held in Vancouver, Canada, 31 May-3 June 2005, pp 731-740.
- Brand EW, Premchitt J, Phillipson HB (1984) Relationship

- between rainfall and landslides, in Hong Kong. In: Proceedings of the 4th International Symposium on Landslides held in Toronto, Canada, 16-21 September 1984, vol. 1, pp 377-384.
- Calcaterra D, de Riso R, Evangelista A, et al. (2004) Slope instabilities in the pyroclastic deposits of the Phlegraean district and the carbonate Apennine (Campania, Italy). In: Proceedings of an International Workshop on Occurrence and Mechanisms of Flows in Natural Slopes and Earthfills held in Sorrento, Italy, 14-16 May 2003, pp 61-75.
- Campbell JE (1990) Dielectric properties and influence of conductivity in soils at one to fifty megahertz. *Soil Science Society American Journal* 54: 332-341. DOI: 10.2136/sssaj1990.03615995005400020006x
- Cascini L, Ferlisi S (2003) Occurrence and consequences of flowslides: a case study. In: Proceedings of an International Conference on Fast Slope Movements – Prediction and Prevention for Risk Mitigation held in Napoli, 11-13 May 2003, vol. 1, pp 85-92.
- Chleborad AF, Baum RL, Godt JW (2008) A prototype system for forecasting landslides in the Seattle, Washington, area. *Reviews in Engineering Geology* 20: 103-120. DOI: 10.1130/2008.4020(06)
- IPCC (Intergovernmental Panel on Climate Change) (2011) *Climate Change 2007: The Physical Science Basis*. Solomon S, Qin D, Manning M, et al. (Eds.), Contribution of Working Group I to the Fourth Assessment Report of the Intergovernmental Panel on Climate Change. Cambridge University Press, Cambridge, UK and New York, USA. Available online: http://www.ipcc.ch/publications_and_data/publications_ipcc_fourth_assessment_report_wg1_report_the_physical_science_basis.htm (Accessed on 15 June 2012)
- Comegna L, Damiano E, Greco R, et al. (2013) Effects of the vegetation on the hydrological behavior of a loose pyroclastic deposit. *Procedia Environmental Sciences* 19: 922-931. DOI: 10.1016/j.proenv.2013.06.102
- Crosta GB, Dal Negro P (2003) Observation and modelling of soil slip–debris flow initiation processes in pyroclastic deposits: the Sarno 1998 event. *Natural Hazards and Earth System Science* 3: 53-69. DOI: 10.5194/nhess-3-53-2003
- Di Crescenzo G, Santo A (2005) Debris slides–rapid earth flows in the carbonate massifs of the Campania region (Southern Italy): morphological and morphometric data for evaluating triggering susceptibility. *Geomorphology* 66: 255-276. DOI: 10.1016/j.geomorph.2004.09.015
- Faella C, Nigro E (2003) Dynamic impact of the debris flows on the constructions during the hydrogeological disaster in Campania-1998: failure mechanical models and evaluation of the impact velocity. In: Proceedings of an International Conference on Fast Slope Movements – Prediction and Prevention for Risk Mitigation held in Napoli, Italy, 11-13 May 2003, pp 179-186.
- Flentje PN, Chowdhury RN, Tobin P, et al. (2005) Towards real-time landslide risk management in an urban area. In: Proceedings of an International Conference on Landslide Risk Management held in Vancouver, Canada, 31 May-3 June 2005, pp 741-751.
- Fredlund DG, Rahardjo H (1993) *Handbook on Soil Mechanics for Unsaturated Soils*. In: Wiley-Interscience Publication, John Wiley & Sons, New York, NY, USA.
- Gasparini P, Manfredi G, Zschau J (2007). Earthquake early warning systems. In: Gasparini P, Manfredi G and Zschau J (Eds.), Springer, Berlin, Heidelberg, Germany.
- Greco R (2006) Soil water content inverse profiling from single TDR waveforms. *Journal of Hydrology* 317: 325-339. DOI: 10.1016/j.jhydrol.2005.05.02
- Greco R, Guida A (2008) Field measurements of topsoil moisture profiles by vertical TDR probes. *Journal of Hydrology* 348(3-4): 442-451. DOI: 10.1016/j.jhydrol.2007.10.013
- Greco R, Guida A, Damiano E, et al. (2010) Soil water content and suction monitoring in model slopes for shallow flowslides early warning applications. *Physics and Chemistry of the Earth* 35: 127-136. DOI: 10.1016/j.pce.2009.12.003
- Greco R, Comegna L, Damiano E, et al. (2013) Hydrological modelling of a slope covered with shallow pyroclastic deposits from field monitoring data. *Hydrology and Earth System Sciences* 17: 4001-4013. DOI: 10.5194/hess-17-4001-2013
- Greco R, Comegna L, Damiano E, et al. (2014) Conceptual hydrological modeling of the soil-bedrock interface at the bottom of the pyroclastic cover of Cervinara (Italy). *Procedia Earth and Planetary Science* 9: 122-131. DOI: 10.1016/j.proeps.2014.06.007
- Guadagno FM, Forte R, Revellino P, et al. (2005) Some aspects of the initiation of debris avalanches in the Campania region: the role of morphological slope discontinuities on the development of failure. *Geomorphology*, 66: 237-254. DOI: 10.1016/j.geomorph.2004.09.024
- Iten M, Puzrin AM (2009) BOTDA road-embedded strain sensing system for landslide boundary localization. In: Proceedings of the 16th Annual International Symposium on Smart Sensor Phenomena, Technology, Networks, and Systems held in San Diego, USA, 9-12 March, 2009.
- Iwamoto M (1990) Standard amount of rainfall for warning from debris disaster. In: Proceedings of the 6th International Conference Field Workshop on Landslides ALPS 90 held in Milan, Italy. pp 77-88.
- Keefer DK, Wilson RC, Mark RK, et al. (1987) Real-time landslide warning during heavy rainfall. *Science* 238: 921-925. DOI: 10.1126/science.238.4829.921
- Malicki MA, Plagge R, Roth CH (1996) Improving the calibration of dielectric TDR soil moisture determination taking into account the solid soil. *European Journal of Soil Science* 47: 357-366. DOI:10.1111/j.1365-2389.1996.tb01409.x
- Niklès M, Thévenaz L, Robert P (1997) Brillouin gain spectrum characterization in single-mode optical fibers. *Journal Lightwave Technology* 15 (10): 1842-1851. DOI: 10.1109/50.633570
- Olivares L (2001) Static liquefaction: an hypothesis for explaining transition from slide to flow in pyroclastic soils. In: Proceedings of the 14th International Satellite Conference on Transition from Slide to Flow–Mechanisms and Remedial Measure held in Trabzon, Turkey, 25-26 August 2001., pp 177-191.
- Olivares L, Damiano E (2007). Post-failure mechanics of landslides: a laboratory investigation of flowslides in pyroclastic soils. *Journal of Geotechnical and Geoenvironmental Engineering*, ASCE 133(1): 51-62. DOI: 10.1061/(ASCE)190-0241(2007)133:1(51)
- Olivares L, Damiano E, Greco R, et al. (2009) An instrumented flume to investigate the mechanics of rainfall-induced landslides in unsaturated granular soils. *Geotechnical Testing Journal* 32(2): 108-118. DOI: 10.1520/GTJ101366
- Olivares L, Picarelli L (2003) Shallow flowslides triggered by intense rainfalls on natural slopes covered by loose unsaturated pyroclastic soils. *Géotechnique* 53(2): 283-288. DOI: 10.1680/geot.2003.53.2.283
- Olivares L, Picarelli L (2006) Modelling of flowslides behaviour for risk mitigation. In: Proceedings of the 6th International Conference on Physical Modelling in Geotechnics held in Hong Kong, 4-6 August 2006, 1, pp 99-113.
- Ortigao B, Justi MG (2004) Rio-Watch: the Rio de Janeiro landslide alarm system. *Geotechnical News* 22 (3): 28-31.
- Pagano L, Picarelli L, Rianna G, Urciuoli G (2010) A simple numerical procedure for timely prediction of precipitation-induced landslides in unsaturated pyroclastic soils. *Landslides* 7(3): 273-289. DOI: 10.1007/s10346-010-0216-x
- Picarelli L (2009) Conoscere per prevedere (dall'equilibrio limite alla meccanica dei pendii). Arrigo Croce Lecture, *Rivista Italiana di Geotecnica*, XLIII(4): 12-68.
- Picarelli L, Evangelista A, Rolandi G, et al. (2006) Mechanical properties of pyroclastic soils in Campania Region. In: Proceedings of the 2nd International Workshop on

- Characterisation and Engineering Properties of Natural Soils, held in Singapore, 5-7 December 2006, 4, pp 2331-2384.
- Picarelli L, Versace P, Olivares L, et al. (2009) Prediction of rainfall-induced landslides in unsaturated granular soils for setting up of early warning systems. In: Proceedings of the International Forum on Landslide Disaster Management held in Hong Kong, 10-12 December 2007, 1, pp 643-665.
- Picarelli L, Zeni L (2009) Discussion to "Test on application of distributed fiber optic sensing technique into soil slope monitoring" by B.J. Wang, K. Lee, B. Shi and J.Q. Wei. *Landslides* 6(4): 361-363. DOI: 10.1007/s10346-009-0169-0
- Pirone M, Damiano E, Picarelli L, et al. (2012) Groundwater-atmosphere interaction in unsaturated pyroclastic slopes at two sites in Italy. *Rivista Italiana di Geotecnica* 3/2012: 29-49.
- Pirone M, Papa R, Nicotera MV, et al. (2014) Evaluation of the hydraulic hysteresis of unsaturated pyroclastic soils by in situ measurements. *Procedia Earth and Planetary Science* 9: 163-170. DOI: 10.1016/j.proeps.2014.06.014
- Poulos SJ (1981) The steady state of deformation. *Journal of Geotechnical Engineering Division ASCE* 107: 553-561.
- Ramo S, Whinnery J, Van Duzer T (1994) *Fields and waves in communication electronics*. Wiley Press, New York, USA.
- Regalado CM, Munoz Carena R, Socorro AR, et al. (2003) Time domain reflectometry models as a tool to understand the dielectric response of volcanic soils. *Geoderma* 117: 313-330. DOI: 10.1016/S0016-7061(03)00131-9
- Rolandi G, Bellucci F, Heizler MT, et al. (2003) Tectonic controls on the genesis of ignimbrites from the Campanian Volcanic Zone, southern Italy. *Mineralogy and Petrology* 79: 3-31. DOI: 10.1007/s00710-003-0014-4
- Sassa K, Picarelli L, Yin YP (2008) Monitoring, prediction and early warning. In: Proceedings of the 1st World Landslide Forum on Disaster Risk Reduction held in Tokyo, 19-21 November 2008, pp 351-375.
- Sladen JA, D'Hollander RD, Krahn J (1985) The liquefaction of sand, a collapse surface approach. *Canadian Geotechnical Journal* 22(4): 564-578. DOI: 10.1139/t85-076
- Sorbino G, Nicotera MV (2013) Unsaturated soil mechanics in rainfall-induced flow landslides. *Engineering Geology* 165: 105-132.
- Topp GC, Davis JL, Annan AP (1980) Electromagnetic Determination of Soil Water Content: Measurement in Coaxial Transmission Lines. *Water Resources Research* 16: 574-582. DOI: 10.1029/WR016i003p00574
- Wiley TJ (2000) Relationship between rainfall and debris flows in western Oregon. *Oregon Geology* 62 (2): 27-43.
- Wilson RC, Mark RK, Barbato G (1993) Operation of a real-time warning system for debris flows in the San Francisco Bay area, California. In: Proceedings of the Hydraulics Division Conference, ASCE, vol. 2, pp 1908-1913.